A simpler method of deuteration was the catalytic exchange of deuterium between acetone-d_6 and the cyclic ketones directly in the NMR tube. As catalyst traces of HCl gas were used, this method yields mixtures of mono-, di-, tri- and tetradeuterated compounds which can, however, be distinguished in most cases. A third method of deuteration was the exchange catalyzed by neutral Al_2O_3. For this purpose the ketone was dissolved in acetone-d_6 and fed through a small capillary filled with Al_2O_3 with a contact time of about 1 min. The spectroscopic results for the monodeuterated compounds were not influenced by the method of the deuteration.

NMR Measurements. The room-temperature 100.6-MHz ^{13}C NMR spectra were taken at 303 K on a Bruker AM-400 spectrometer equipped with an 256K Aspect 3000 computer using acetone-d_6 solutions or in some cases $CDCl_3$, with small detectable difference of the deuterium isotope effects. The measurements were always performed on mixtures of labeled and unlabeled compounds as given above. The spectral width was set at narrow as possible and separate for the carbonyl and aliphatic regions, typically between 1000 and 4000 Hz. Zero filling to 64K gave a digital resolution better than 0.1 Hz/pt after the Fourier transform. Gaussian multiplication was used to increase the resolution.

The force-field calculations were performed on an IBM-AT personal computer with mathematical coprocessor and EGA graphic equipment.

Acknowledgment. This work was supported by the Fonds der Chemischen Industrie and the Deutsche Forschungsgemeinschaft (Be 631/6-3).

Proton On-Resonance Rotating Frame Spin-Lattice Relaxation Measurements of B and Z Double-Helical Oligodeoxyribonucleotides in Solution

Yu-Sen Wang and Satoshi Ikuta*

Contribution from the Department of Chemistry, Illinois Institute of Technology, Chicago, Illinois 60616. *Received March 25, 1988*

Abstract: A method is proposed to account for proton on-resonance rotating frame spin-lattice relaxation, $R_{1\rho}$, of biological macromolecules in solution. The $R_{1\rho}$ measurements detect motions in a time range of the inverse of the frequency of the spin-locking field, ω_1 (tens of kilohertz). The $R_{1\rho}$ time scale (microsecond) is significantly different from those accessible by the usual solution ^1H NMR techniques (nanosecond for R_1 and NOE and millisecond for R_2 and line-shape analysis). The proposed $R_{1\rho}$ method would be conveniently utilized to monitor DNA stiffness in the time range of $1/\omega_1$. As an application of the $R_{1\rho}$ measurements, internal motions of B- and Z-type d(CG)$_3$ are studied in 2 M $NaClO_4$ solution. Results of the $R_{1\rho}$ measurements demonstrate that both the B- and Z-d(CG)$_3$ possess the internal motions in the time range of $1/\omega_1$, but the magnitude of $R_{1\rho(ex)}$ for the B- and Z-d(CG)$_3$ is significantly different. The Z-d(CG)$_3$ has $R_{1\rho(ex)}$ a factor of 2- and 3-fold larger than the B-d(CG)$_3$ under identical conditions at this time scale.

It has been recognized that the structure of DNA molecules must be considered dynamic rather than static. Internal mobilities may play pivotal roles in the recognition of the DNA sequences and in the expression of their biological functions.[1] Along this line, various NMR relaxation studies on large fragments of DNA molecules have been conducted and have shown that double-stranded DNAs are not rigid, but experience fluctuations in the base and phosphate backbone.[2-6] Recently, the internal mobilities of the B and Z DNA have been studied by a number of biophysical chemists to demonstrate the sequence dependence of conformational change and dynamics.

With respect to the internal motions of the DNA molecules, contradictory results between the B and Z DNA have been reported. For example, fluorescent polarization measurements[7] indicate that the Z-form DNA is considerably more mobile than the B form, but light-scattering measurements[8] support the opposite. The proton-exchange rates of the Z DNA are much slower than those of the B DNA.[9,10] Recent NMR relaxation studies[11] show that the internal motions are similar or comparable in both conformations. These discrepancies might arise from the comparison of the internal motions occurring at different time scales.

Various ^1H NMR techniques have been used to monitor the dynamics of DNA in solution. The measurements of spin-lattice relaxation (R_1), sometimes referred to as laboratory frame spin-lattice relaxation, and NOE are the most widely used. These are sensitive to the motions characterized by the Larmor frequency of the observed nuclei which is of the order of 10^{-9}-10^{-10} s (nanosecond) for ^1H on modern high-resolution NMR spectrometers. The spin-spin relaxation measurements (R_2) and line-shape analyses, on the other hand, provide information on the exchange lifetimes in the chemical shift difference time scale which is of the order of 10^{-3} s (millisecond).

By contrast, on-resonance spin-lattice relaxation rates in the rotating frame, $R_{1\rho}$, are the rate constants characterizing the decay of the magnetization of the signals spin-locked by the radio frequency field (rf), $\omega_1 = \gamma B_1$, rotating in the plane normal to the static magnetic field, B_0. Consequently, the observed relaxation rates, $R_{1\rho(obsd)}$, depend on the spectral density governed by ω_1 used in the experiments. The internal motions occurring at or near the frequency of ω_1 fields (tens of kilohertz) can contribute to the

(1) Jardetzky, O. *Acc. Chem. Res.* **1981**, *14*, 291-298.
(2) Hogan, M. E.; Jardetzky, O. *Proc. Natl. Acad. Sci. U.S.A.* **1979**, *76*, 6341-6345.
(3) Bolton, P. H.; James, T. L. *J. Am. Chem. Soc.* **1980**, *102*, 25-31.
(4) Early, T. A.; Kearns, D. R. *Proc. Natl. Acad. Sci. U.S.A.* **1979**, *76*, 4165-4169.
(5) Shindo, H. *Biopolymers* **1980**, *19*, 509-522.
(6) Bolton, P. H.; James, T. L. *J. Phys. Chem.* **1979**, *83*, 3359-3366.
(7) Ashikawa, I.; Kinosita, K.; Ikegami, A. *Biochim. Biophys. Acta* **1984**, *782*, 87-93.
(8) Thomas, T. J.; Bloomfield, V. A. *Nucleic Acids Res.* **1983**, *11*, 1919-1930.
(9) Pilet, J.; Leng, M. *Proc. Natl. Acad. Sci. U.S.A.* **1982**, *79*, 26-30.
(10) Mirau, P. A.; Kearns, D. R. *Proc. Natl. Acad. Sci. U.S.A.* **1985**, *82*, 1594-1598.
(11) Mirau, P. A.; Behling, R. W.; Kearns, D. R. *Biochemistry* **1985**, *24*, 6200-6211.

0002-7863/89/1511-1243$01.50/0

relaxation mechanisms. Therefore, the $R_{1\rho}$ measurements can be used to probe the internal motions in a time range (microsecond) that was not previously accessible by measurements of R_1 and R_2.

Although the phenomenon of $R_{1\rho}$ has been known for many years,[12] and the $R_{1\rho}$ measurements have been used to monitor the motions of the solid polymers,[13] few studies of $R_{1\rho}$ in solution have been reported. Deverell et al.[14] reported the study of the chair-to-chair isomerization of cyclohexane by the $R_{1\rho}$ measurements. Bleich and Glasel used the $R_{1\rho}$ technique for the studies of internal mobilities of glycylglycine[15] and enkephalin.[16] For the size of molecules in these studies ($\omega\tau_c \ll 1$), the dipolar contribution in the rotating frame, $R_{1\rho(dd)}$, equals that in the laboratory frame, R_1. In recent years, Kopple and co-workers have studied the internal mobilities of cyclic peptides by the $R_{1\rho}$ techniques.[17-19] An excellent procedure has been developed to obtain the exchange contribution for the molecules of this size ($\omega\tau_c \sim 1$). The exchange lifetimes of the internal motions in the range of 7–23 μs[19] were observed for the cyclic octapeptides in solution and were faster than the time scale accessible by the usual R_2 or line-shape analysis. These studies demonstrated the feasibility of $R_{1\rho}$ to monitor the microsecond motions.

However, the procedures developed in the past are hardly applicable for the evaluation of the exchange contribution of macromolecules ($\omega\tau_c \gg 1$) due to (i) the fact that the dipolar interaction contribution $R_{1\rho(dd)}$ is not equal to $R_{1(dd)}$, (ii) the use of nonselective spin–lattice relaxation, and (iii) the presence of a spin–diffusion. To overcome these complications, we propose a procedure for the evaluation of the conformational exchange contributions, $R_{1\rho(ex)}$, using the initial recovery rates of the selective spin–lattice relaxation. The proposed method extends the $R_{1\rho}$ measurements that had been developed for molecules of small[12,14-16] and intermediate[17-19] sizes to macromolecules.

This method would be conveniently utilized to monitor the stiffness and elastic properties of DNA. DNA bending motions are essential to construct nucleosome particles in chromatin and occur in the microsecond time scale.[20] DNA stiffness may be significant when a protein must bend the DNA molecule to form its complex.[21]

James et al.[3,6,22] developed an off-resonance rotating frame spin–lattice relaxation ($T_{1\rho}^{off}$) for the ^{13}C and ^{31}P nuclei to study the dynamics of various protein, DNA, and RNA molecules. The $T_{1\rho}^{off}$ measurements utilized the rf field applied far away from the signal of interest and used a ratio of peak intensities in the presence and absence of an off-resonance rf field. The ratio was related to both $1/T_1$ and $1/T_{1\rho}^{off}$.

$R_{1\rho}$ described in this text is an on-resonance rotating frame spin–lattice relaxation: the carrier is placed on the frequency of signals of interest and the decays of the magnetization are monitored during the spin-locking period. Therefore, the relaxation mechanism and interpretation of the data for the $R_{1\rho}$ measurements differ from those for the $T_{1\rho}^{off}$ measurements.

In this paper, we present the proposed procedure to account for the proton on-resonance rotating frame spin–lattice relaxation for studying the dynamics of macromolecules in solution and describe the first application of this method to monitor the internal mobilities of B- and Z-type oligodeoxyribonucleotides in solution.

Experimental Section

Materials. The synthesis of $d(CG)_3$ was carried out by the published procedure.[23] After the synthesis, $d(CG)_3$ was purified by the procedure described previously.[24] For the preparation of the NMR sample, 73 OD units of $d(CG)_3$ at 260 nm were dissolved in 0.3 mL of D_2O containing 10 mM sodium phosphate, 0.1 M NaCl, and 2 M $NaClO_4$ at pH = 6.6.

NMR Measurements. NMR spectra and relaxation data were obtained on a Nicolet NT-300 spectrometer. Nonselective spin–lattice relaxation rates, R_1^{NS}, were measured by the inversion recovery techniques (180°–τ–90°–Acq). Selective spin–lattice relaxation measurements, R_1^S, were carried out by a selective 180° (26-ms) soft pulse from the decoupler to the signals of interest. After a delay time, τ, the 90° pulse was applied for observation purposes and the resulting FIDs were collected and Fourier transformed. Peak heights were measured from the spectra recorded at different delay times, τ. The initial recovery rates, R_1^{IS}, of the selective spin–lattice relaxation measurements were extracted from the initial decay of the magnetization in the plot of ln ($M_\infty - M_t$) vs delay times, τ.

Rotating frame spin–lattice relaxation rates, $R_{1\rho}$, were measured by the spin-locking pulse sequence, $90°_x$–$t(SL)_y$–Acq, where (SL) denotes spin-locking and t is the spin-locking time. The spin-locking was achieved at an rf field of 5000 Hz, and the relaxation rates were measured with different lengths of spin-locking time, t. The peak intensities were fitted to $I = I_0 \exp\{-t/T_{1(\rho)}\} + I_p$, where I_p is the residual signal at long spin-locking times, by a nonlinear least-squares analysis to obtain $T_{1\rho}$ ($1/R_{1\rho}$).

Excitation and spin-locking powers were obtained from the low-power transmitter of the spectrometer with an ENI 10-W linear amplifier. The carrier frequency was placed in the middle of the signals of interest within 100 Hz. It has been previously determined that an offset up to 200 Hz has no observable effect on $R_{1\rho}$.[19] Under this condition, the Hartman–Hahn effects, which were pointed out by Bax et al.,[25] are not significant. Errors have been estimated to be less than 5% for the R_1 and the $R_{1\rho}$ measurements. Chemical shifts (ppm) were reported relative to the chemical shift of the DSS (2,2-dimethyl-2-silapentane-5-sulfonate) signal.

Theory

A number of physical mechanisms can contribute to the observed (overall) rotating frame spin–lattice relaxation rates, $R_{1\rho(obsd)}$. However, the major contributors are the dipole–dipole interactions between the observed and neighboring protons for a proton directly attached to a carbon atom (the C–H in DNA). An additional relaxation mechanism is the modulation of chemical shift differences when nuclei exchange between sites, if present. This effect will be maximal when the exchange rates are near the frequency of the spin-locking field ($\omega_1 = \gamma B_1$). Since the C–H protons are nonexchangeable, the exchange contribution, $R_{1\rho(ex)}$, results only from the internal motions, such as conformational exchange or transient conformational flexibilities. Thus, the observed rates, $R_{1\rho(obsd)}$, can be expressed as a sum of the contributions from the dipolar interactions, $R_{1\rho(dd)}$, and the exchange contributions, $R_{1\rho(ex)}$, as follows:[15]

$$R_{1\rho(obsd)} = R_{1\rho(dd)} + R_{1\rho(ex)} \quad (1)$$

$R_{1\rho(ex)}$ contains information regarding the internal motions. We take the exchange contribution, $R_{1\rho(ex)}$, as a measure of the internal mobilities because it contains effects from the exchange rates and chemical shift differences between sites. The evaluation of $R_{1\rho(ex)}$ of DNA is one of the objectives in this study. It is evident from eq 1 that, in order to obtain $R_{1\rho(ex)}$, $R_{1\rho(dd)}$ needs to be evaluated.

(12) Strange, J. H.; Morgan, R. E. *J. Phys. C.* **1970**, *3*, 1999–2011.
(13) (a) Douglass, D. C. In *Polymer Characterization by ESR and NMR*; Woodward, A. E., Bovey, F. A., Eds.; ACS Symposium Series 142; American Chemical Society: Washington, DC, 1980; pp 147–168. (b) Schaefer, J.; Sefcic, M. D.; Stejskal, E. O.; McKay, R. A.; Dixon, W. T.; Cais, R. E. *Macromolecules* **1984**, *17*, 1107–1118.
(14) Deverell, C.; Morgan, R. E.; Strange, J. H. *Mol. Phys.* **1970**, *18*, 553–559.
(15) Bleich, H. E.; Glasel, J. A. *Biopolymers* **1978**, *17*, 2445–2457.
(16) Bleich, H. E.; Day, A. R.; Freer, R. J.; Glasel, J. A. *Biochem. Biophys. Res. Commun.* **1979**, *87*, 1146–1153.
(17) (a) Kopple, K. D.; Wang, Y.-S. In *Peptides*, Proceedings of the 9th American Peptide Symposium; Deber, C. M., Hruby, V. J., Kopple, K. D., Eds.; Pierce Chemical Co.: Rockford, IL, 1985; pp 133–136. (b) Kopple, K. D.; Wang, Y.-S. In *Peptides*, Proceedings of the 19th European Peptide Symposium; Theodropoulos, D., Ed.; Walter de Gruyter and Co.: Berlin, 1987; pp 283–286. (c) Kopple, K. D.; Wang, Y.-S. *Int. J. Peptide Protein Res.*, in press.
(18) Kopple, K. D.; Bhandary, K. K.; Kartha, G.; Wang, Y.-S.; Parameswaran, K. N. *J. Am. Chem. Soc.* **1986**, *108*, 4637–4642.
(19) Kopple, K. D.; Wang, Y.-S.; Cheng, A. G.; Bhandary, K. K. *J. Am. Chem. Soc.* **1988**, *110*, 4168–4176.
(20) (a) Finch, J. T.; Lutter, L. C.; Rhodes, D.; Brown, R. S.; Rushton, B.; Klug, A. *Nature* **1977**, *269*, 29–36. (b) Hogan, M.; Wang, J.; Austin, R. H.; Monitto, C. L.; Hershkowitz, S. *Proc. Natl. Acad. Sci. U.S.A.* **1982**, *79*, 3518–3522.
(21) Hogan, M.; LeGrange, J.; Austin, R. H. *Nature* **1983**, *304*, 752–754.
(22) (a) James, T. L. *J. Magn. Reson.* **1980**, *39*, 141–153. (b) James, T. L.; Matson, G. B.; Kuntz, I. D. *J. Am. Chem. Soc.* **1978**, *100*, 3590–3594.
(23) Tan, Z. K.; Ikuta, S.; Huang, T.; Dugaiczyk, A.; Itakura, K. *Cold Spring Harbor Symp. Quant. Biol.* **1983**, *47*, 383–391.
(24) Ikuta, S.; Chattopadhyaya, R.; Dickerson, R. E. *Anal. Chem.* **1984**, *56*, 2253–2256.
(25) Bax, A.; Davis, D. G. *J. Magn. Reson.* **1985**, *63*, 207–213.

The following sections, A–C, are the basis for obtaining $R_{1\rho(dd)}$.

(A) Rotating Frame Dipolar Relaxation. For a two-spin system (spin H and 1), $R_{1\rho(dd)}$ for unlike spins ($\Delta\omega_{H-1} = \omega_H - \omega_1 > R_2$)[26] can be expressed in terms of the spectral densities, $J_n(\omega)$, as follows:[27]

$$R_{1\rho(dd)} = (\hbar^2\gamma_H^2\gamma_1^2)/4r^6[4J(\omega_1) + J_0(\omega_H - \omega_1) + 3J_1(\omega_H) + 6J_1(\omega_1) + 6J_2(\omega_H + \omega_1)] \quad (2)$$

where γ_H and γ_1 are the gyromagnetic ratios for spins H and 1 ($\omega_H = \omega_1$ in this case), r is the H–1 internuclear distance, ω_1 is the spin-locking field, and $\hbar$ is Planck's constant divided by 2π.

Oligodeoxyribonucleotides can be approximated as isotropic rotors with correlation times τ_c (usually at a nanosecond time scale) and have spectral densities of $J_n(\omega) = (\tau_c/5)[1 + (\omega\tau_c)^2]^{-1}$. The overall tumbling of the molecules at this time scale contributes to both $R_{1\rho}$ and R_1. However, the internal motions occurring in the $R_{1\rho}$ time range (microsecond time scale) contribute only to $R_{1\rho}$, but not to R_1.

$R_{1\rho(dd)}$ cannot be directly computed because the effective interproton distance, r, between the proton and neighboring protons is not known for conformationally mobile molecules. However, $R_{1\rho(dd)}$ can be obtained from R_1 and a ratio $(R_{1\rho}/R_1)$.[18]

(B) Laboratory Frame Dipolar Relaxation. For the nonexchangeable C–H protons, the spin–lattice relaxation rates are dominated by dipolar interactions. For a two-spin system, if spin H is selectively excited, the selective spin–lattice relaxation rates, R_1^S, are given by the following equation:[28]

$$R_1^S = \hbar^2\gamma_H^2\gamma_1^2/2r^6[J_0(\omega_H - \omega_1) + 3J_1(\omega_H) + 6J_2(\omega_H + \omega_1)] \quad (3)$$

where the superscript S denotes the selective spin–lattice relaxation rates.

The initial rates of the magnetization recovery after the selective inversion of the spin H are given by[28]

$$R_1^{IS} = \hbar^2\gamma_H^2\gamma_1^2/2r^6[J_0(\omega_H - \omega_1)] \quad (4)$$

where the superscript, IS, denotes the initial rates of the magnetization recovery following the selective excitation of the signal. As relaxation proceeds, the populations of the H and 1 spins equalize and single (J_1) and double quantum (J_2) terms in eq 3 become dominant. This leads to the smaller relaxation rates, with the resulting rates being expressed as follows:[28]

$$R_1^{NS} = \hbar^2\gamma_H^2\gamma_1^2/2r^6[3J_1(\omega_H) + 12J_2(\omega_H + \omega_1)] \quad (5)$$

Equation 5 is the same for the recovery of the magnetization in the two-spin system where both spins are simultaneously inverted. The superscript, NS, denotes nonselective relaxation rates.

(C) Evaluation of Rotating Frame Dipolar Contribution. For evaluating $R_{1\rho(dd)}$ of macromolecules, the ratio $[R_{1\rho(dd)}/R_1]$ is taken, leading to the elimination of the distance dependent term, r^6. The ratio depends on the two constants, γB_0 and γB_1, and a variable, τ_c. $R_{1\rho(dd)}$ can be obtained as the product of R_1 and the ratio.

With respect to R_1 of macromolecules, two complications exist as follows: (i) the use of R_1^{NS} and (ii) the presence of the spin–diffusion. Figure 1 shows plots of theoretical values of the ratios $[R_{1\rho(dd)}/R_1^{NS}$ and $R_{1\rho(dd)}/R_1^S]$ at $\gamma B_0 = 300$ MHz and $\gamma B_1 = 5000$ Hz as a function of τ_c. For small molecules ($\tau_c \leq 10^{-10}$ s), both ratios are unity. As τ_c exceeds 10^{-9} s, the ratio $[R_{1\rho(dd)}/R_1^{NS}]$ rises rapidly. In contrast, at $\omega\tau_c \geq 1$ the ratio $[R_{1\rho(dd)}/R_1^S]$ increases smoothly with an increase in τ_c and reaches a finite value of 2.5. Therefore, R_1^S should be used to evaluate dipolar contributions instead of R_1^{NS}.

The spin–diffusion is commonly encountered when relaxation rates of the macromolecules are concerned. Useful information can only be extracted from the initial recovery rates. Based on the analysis of the two complications, only the initial recovery rates, R_1^{IS}, of the selective spin–lattice relaxation measurements can be used for the evaluation of the relaxation data of macromolecules. Given a knowledge of τ_c, the ratio $[R_{1\rho(dd)}/R_1^{IS}]$ will be calculated. Therefore, $R_{1\rho(dd)}$ can be indirectly obtained from R_1^{IS} and τ_c. The overall tumbling time, τ_c, of oligodeoxyribonucleotides can be readily calculated by the Stokes–Einstein relation, assuming that short DNA duplexes act as isotropic rotors. This procedure has been proven to provide a reasonable approximation to predict the overall tumbling time for short DNA oligomers.[29]

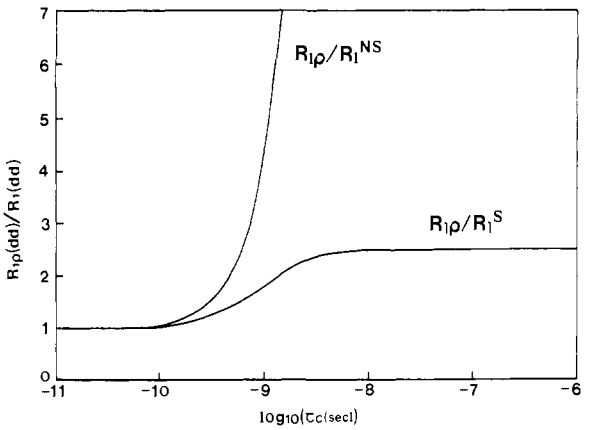

Figure 1. Theoretical values of the ratios $[R_{1\rho(dd)}/R_1^{NS}$ and $R_{1\rho(dd)}/R_1^S]$ at constant field strengths, $\gamma B_0 = 300$ MHz and $\gamma B_1 = 5000$ Hz as a function of τ_c.

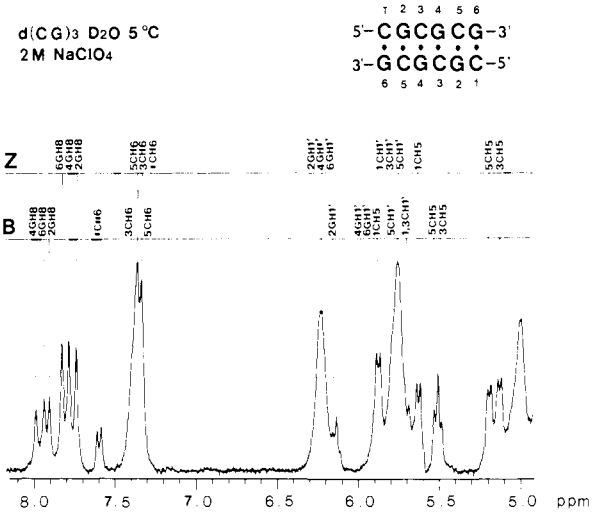

Figure 2. The ^{1}H NMR spectrum of the nonexchangeable protons of the B- and Z-d(CG)$_3$ at 5 °C in D_2O. The d(CG)$_3$ has 4.2 mM strand concentration in 10 mM sodium phosphate, 0.1 M NaCl, and 2 M $NaClO_4$, at pH = 6.6. Assignments of the signals to the specific protons are given above the lines.

Results

Three major points of this paper are as follows. (i) A procedure is proposed to account for the proton on-resonance rotating frame spin–lattice relaxation to study the internal mobilities of biological macromolecules in solution. (ii) The $R_{1\rho}$ measurements demonstrate that the *B-type* structure of d(CG)$_3$ [B-d(CG)$_3$] and the *Z-type* structure of d(CG)$_3$ [Z-d(CG)$_3$] in 2 M $NaClO_4$ solution possess the internal motions in the time range of $1/\omega_1$. However, (iii) exchange contributions for the B- and Z-d(CG)$_3$ are significantly different; those for the Z-d(CG)$_3$ are 2–3 times as large as those for the B-d(CG)$_3$ at this time scale.

Resonance Assignments. The ^{1}H spectra of the aromatic and anomeric H1′ proton region of d(CG)$_3$ in 2 M $NaClO_4$ solution at 5 °C along with the sequence and numbering system used are

(26) Assa-Munt, N.; Granot, J.; Behling, R. W.; Kearns, D. R. *Biochemistry* **1984**, *23*, 944–955.
(27) Harris, R. K. *Nuclear Magnetic Resonance Spectroscopy*; Pitman Publishing Inc.: Marshfield, MA, 1983.
(28) Abragam, A. *The Principles of Nuclear Magnetism*; Oxford University Press: London, 1961.
(29) Clore, G. M.; Gronenborn, A. M. *FEBS Lett.* **1984**, *172*, 219–225.

Table I. Proton Chemical Shifts (ppm) of the Representative Resonances in the B- and Z-d(CG)$_3$ in 0.1 M NaCl, 2 M $NaClO_4$, and 10 mM Sodium Phosphate at 5 °C, pH = 6.6

		B-d(CG)$_3$			Z-d(CG)$_3$		
		GH8/CH6	CH5	GH1′/CH1′	GH8/CH6	CH5	GH1′/CH1′
1	C	7.58	5.86	5.68	7.33	5.61	5.74
2	G	7.88		6.12	7.72		6.21
3	C	7.38	5.49	5.68	7.34	5.12	5.74
4	G	7.96		5.86	7.76		6.21
5	C	7.34	5.50	5.74	7.37	5.18	5.74
6	G	7.91		5.86	7.80		6.21

Table II. Laboratory Frame Spin–Lattice Relaxation Rates, R_1^{IS} and R_1^{NS}, for the Base Protons of the B- and Z-d(CG)$_3$ in 2 M $NaClO_4$ at 5 °C

	R_1^{IS}, s^{-1}	R_1^{NS}, s^{-1}
B-d(CG)$_3$		
4GH8	4.8	1.00
3/5CH5[a]	3.0	0.78
Z-d(CG)$_3$		
4GH8	4.9	0.51
3CH5	5.0	0.41
5CH5	5.3	0.42

[a] The 3CH5 and 5CH5 (3/5CH5) of the B-d(CG)$_3$ are overlapped.

shown in Figure 2. The assignments of the B- and Z-d(CG)$_3$ are carried out by comparing the NOESY[30] and COSY[31] spectra obtained in 2 M $NaClO_4$ with those in 0 and 4 M $NaClO_4$ solutions at 5 °C (data not shown). Two sets of signals are observed for the corresponding protons of the B-d(CG)$_3$ and Z-d(CG)$_3$ (Figure 2). These signals are well separated and sharp, indicating that the B-to-Z transition is slower than the NMR chemical shift difference time scale. The exchange lifetimes between the B- and Z-d(CG)$_3$ are longer than 3 s under our experimental conditions (see Discussion). The assignments of the signals of interest to the specific protons are given in Figure 2 and are summarized in Table I.

Laboratory Frame Spin–Lattice Relaxation Measurements. The laboratory frame selective spin–lattice relaxation rates, R_1^S, have been measured for the 4GH8, 3CH5, and 5CH5 of the B- and Z-d(CG)$_3$ at 5 °C. An example of the spin–lattice relaxation measurements for the 5CH5 of the Z-d(CG)$_3$ and a semilog plot of its recovery rate are shown in Figure 3A and B, respectively. The data demonstrate that the magnetization of the 5CH5 recovers exponentially within the short delay time (τ = 150 ms), but recovers nonexponentially after that time due to the spin–diffusion.[26]

Values of R_1^{IS} obtained from the initial slopes are 3.0 and ~5.2 s^{-1} for the 3/5CH5, and 4.8 and 4.9 s^{-1} for the 4GH8 of the B- and Z-d(CG)$_3$, respectively. Nonselective spin–lattice relaxation rates, R_1^{NS}, for the 4GH8 of the B- and Z-d(CG)$_3$ are found to be 1.0 and 0.5 s^{-1}, respectively. For comparison purposes, R_1^{IS} and R_1^{NS} for the 3/5CH5 and 4GH8 are listed in Table II.

Rotating Frame Spin–Lattice Relaxation Measurements. The rotating frame spin–lattice relaxation measurements are carried out for the base protons of the internal residues of the B- and Z-d(CG)$_3$ at ω_1 = 5000 Hz. Figure 4A and B show the $R_{1\rho}$ measurements for the 4GH8 and the 3/5CH5 of the B- and Z-d(CG)$_3$, respectively, in D_2O at 5 °C. Semilog plots of the peak intensities vs delay times, t, for the 3/5CH5 of the B-d(CG)$_3$ and the 5CH5 of the Z-d(CG)$_3$ are shown in Figure 4C. $R_{1\rho(obsd)}$ of 11.0 s^{-1} is obtained for the 3/5CH5 of the B-d(CG)$_3$ and that of 24.4 s^{-1} is obtained for the 5CH5 of the Z-d(CG)$_3$. Similarly, $R_{1\rho(obsd)}$ of 17.9 and 24.4 s^{-1} are obtained for the 4GH8 of the B- and Z-d(CG)$_3$, respectively. These data are listed in Table III.

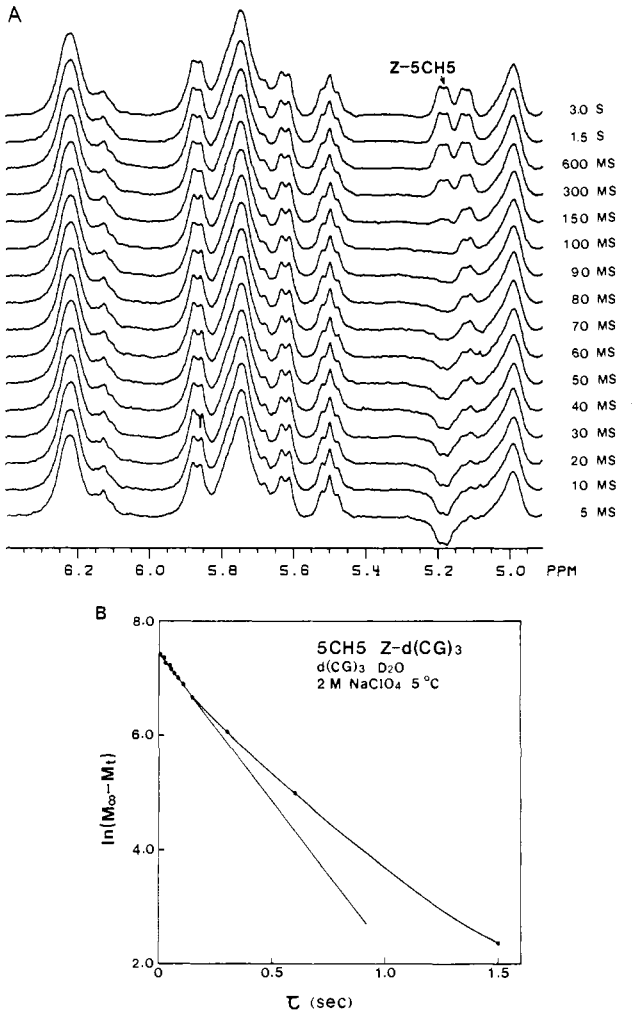

Figure 3. (A) Laboratory frame selective spin–lattice relaxation measurements for the 5CH5 of the Z-d(CG)$_3$ at 5 °C. The 5CH5 is selectively inverted by a soft pulse. (B) A semilog plot of the recovery of the magnetization after the selective inversion of the 5CH5 of the Z-d(CG)$_3$ at 5 °C.

Table III. Rotating Frame Spin–Lattice Relaxation Rates, $R_{1\rho(obsd)}$, Laboratory Frame Spin–Lattice Relaxation Rates, R_1, Ratios, Dipolar Contribution, $R_{1\rho(dd)}$, and Exchange Contribution, $R_{1\rho(ex)}$, for the Base Protons of the B- and Z-d(CG)$_3$ in 2 M $NaClO_4$ at 5 °C

	$R_{1\rho(obsd)}$, s^{-1}	R_1^{IS}, s^{-1}	R[a]	$R_{1\rho(dd)}$, s^{-1}	$R_{1\rho(ex)}$, s^{-1}
B-d(CG)$_3$					
4GH8	17.9	4.8	2.6	12.5	5.4
3/5CH5	11.0	3.0	2.6	7.8	3.2
Z-d(CG)$_3$					
4GH8	24.4	4.9	2.6	12.7	11.7
3CH5	24.4	5.0	2.6	13.0	11.4
5CH5	24.4	5.3	2.6	13.8	10.6

[a] R is the ratio in the dipolar terms between the rotating and laboratory frame relaxation rates, $R = R_{1\rho(dd)}/R_1^{IS}$.

Overall Tumbling Time. The overall tumbling times of the B- and Z-d(CG)$_3$ in 2 M $NaClO_4$ at 5 °C are estimated from the Stokes–Einstein relation by using a viscosity of 1.77 cP.[32] The B-d(CG)$_3$ is approximated as a cylinder with a diameter of 26 Å and a rise per residue of 3.40 Å,[33] while the Z-d(CG)$_3$ is 22 Å and 3.70 Å.[34] The height of the cylinder equals nh, where h is the rise per residue and n is the number of base pairs (n = 6).

(30) Kumar, A.; Ernst, R. R.; Wuthrich, K. *Biochem. Biophys. Res. Commun.* **1980**, *95*, 1.
(31) Nagayama, K.; Kumar, A.; Wuthrich, K.; Ernst, R. R. *J. Magn. Reson.* **1980**, *40*, 321.
(32) The viscosity of 2 M $NaClO_4$ solution at 5 °C is measured by capillary viscometries.
(33) Dickerson, R. E.; Drew, H. R. *J. Mol. Biol.* **1981**, *149*, 761–786.
(34) Wu, H. M.; Dattagupta, N.; Crothers, D. M. *Proc. Natl. Acad. Sci. U.S.A.* **1981**, *78*, 6808–6811.

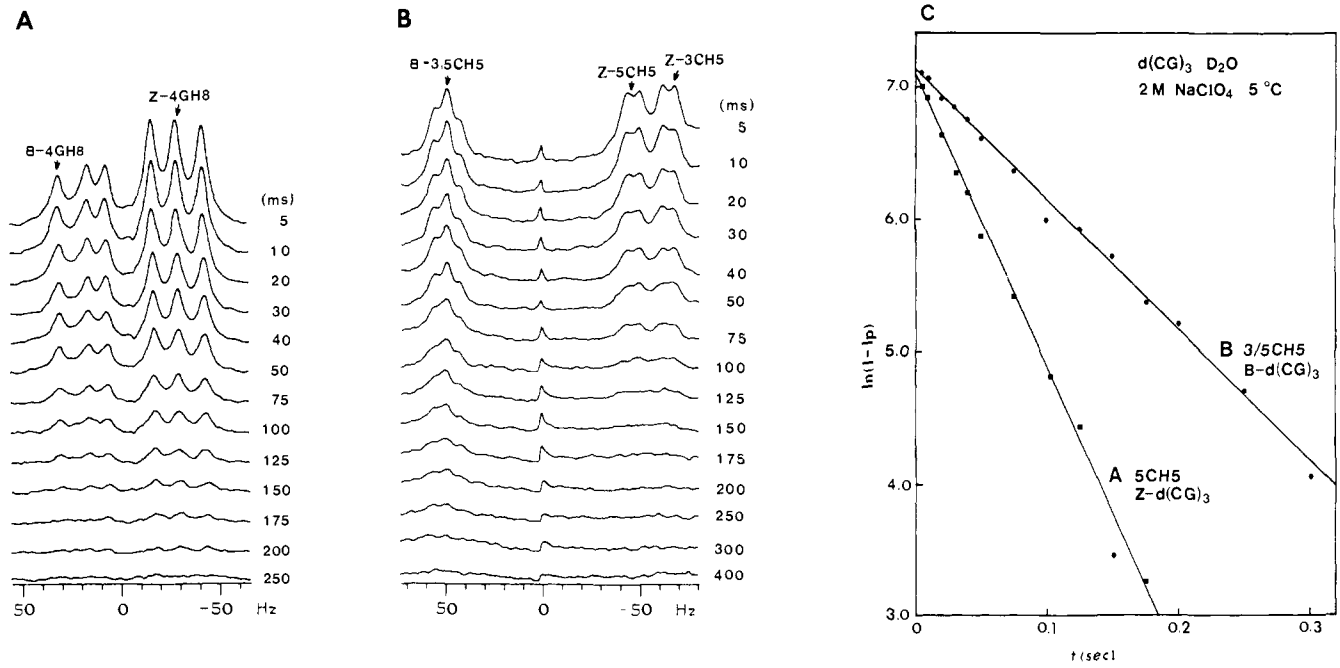

Figure 4. Rotating frame spin-lattice relaxation measurements of (A) the 4GH8 resonance of the B- and Z-d(CG)$_3$ and (B) the 3/5CH5 of the B- and Z-d(CG)$_3$ at 5 °C. The 4GH8 or 3/5CH5 resonances of the B- and Z-d(CG)$_3$ are spin-locked right after the 90° pulse. (C) A semilog plot of the recovery of the rotating frame spin-lattice relaxation of the 3/5CH5 of the B-d(CG)$_3$ and 5CH5 of the Z-d(CG)$_3$ at 5 °C.

The τ_c values calculated for the B- and Z-d(CG)$_3$ in 2 M NaClO$_4$ are 5.0 and 3.9 ns, respectively.

Evaluation of Rotating Frame Dipolar Contribution. From τ_c calculated above, the ratio $[R_{1\rho(dd)}/R_1^{IS}]$ is evaluated at γB_0 = 300 MHz and $\omega_1 = \gamma B_1$ = 5000 Hz. The obtained ratios are 2.56 for the B-d(CG)$_3$ with τ_c = 5.0 ns and 2.59 for the Z-d(CG)$_3$ with τ_c = 3.9 ns. From the ratios, ~2.6, $R_{1\rho(dd)}$ of 12–13 s^{-1} are obtained for the 4GH8 of the B- and Z-d(CG)$_3$. The data are summarized in Table III.

For comparison purposes, we have calculated the ratios using R_1^S and R_1^{NS} instead of R_1^{IS}. The ratios for the B-d(CG)$_3$ with τ_c = 5.0 ns are 2.43 and 68.6 and those for the Z-d(CG)$_3$ with τ_c = 3.9 ns are 2.40 and 42.3, using R_1^S and R_1^{NS}, respectively.

Chemical Exchange. The chemical-exchange contributions, $R_{1\rho(ex)}$, are obtained from the difference in the magnitude between $R_{1\rho(obsd)}$ and $R_{1\rho(dd)}$. $R_{1\rho(ex)}$ of 5.4 and 11.7 s^{-1} are obtained for the 4GH8 of the B- and Z-d(CG)$_3$, respectively. Similarly, $R_{1\rho(ex)}$ of 3.2 and ~11 s^{-1} are obtained for the CH5 of the B- and Z-d(CG)$_3$, respectively, and are listed in Table III. The Z-d(CG)$_3$ has $R_{1\rho(ex)}$, a factor of 2- to 3-fold larger than the B-d(CG)$_3$ under identical conditions.

Discussion

Coexistence of the B- and Z-d(CG)$_3$. Unique features of our experimental system consist of several aspects and are summarized as follows: (i) the B- and Z-d(CG)$_3$ coexist in 2 M NaClO$_4$ at 5 °C, (ii) all relaxation measurements of the B- and Z-d(CG)$_3$ are performed in a single NMR tube under identical conditions, (iii) some of the signals (GH8 and CH5) that are used as probes to monitor the internal motions are well resolved, (iv) the exchange lifetimes of the B-to-Z transition for the d(CG)$_3$ are measured as long as 3 s at *18* °C by the saturation transfer technique,[35] and therefore, (v) the B-to-Z transition does not contribute to the $R_{1\rho}$ relaxation mechanism under our experimental conditions (5 °C). On the basis of these facts, $R_{1\rho(ex)}$ obtained in our experiments reflect only the internal mobilities of the B- and Z-d(CG)$_3$.

Three Regimes. There are three different regimes used to describe the relationship between the size of the molecules and the operating spectrometer frequency, as illustrated in Figure 5. Region 1 is known as the extreme narrowing regime ($\omega\tau_c \ll 1$). $R_{1\rho(ex)}$ can be readily obtained by $R_{1\rho(ex)} = R_{1\rho(obsd)} - R_1^{NS}$,[14-16]

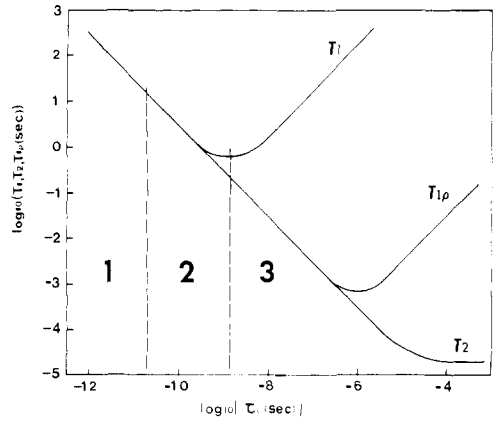

Figure 5. Schematic drawing of the dependence of relaxation times of T_1, T_2, and $T_{1\rho}$ on the correlation time, τ_c. Region 1 is known as the extreme narrowing condition ($\omega\tau_c \ll 1$), while region 2 corresponds to $\omega\tau_c \sim 1$ and region 3 corresponds to $\omega\tau_c \gg 1$.

since $R_{1\rho(dd)} = R_1^{NS}$. Regime 2 includes molecules of the intermediate size ($\omega\tau_c \sim 1$), i.e., oligopeptides and oligosaccharides; $R_{1\rho(dd)}$ significantly differs from R_1^{NS}. For evaluation of the dipolar contribution, $R_{1\rho(dd)}$, Kopple and co-workers[17-19] utilized the ratio $[R_{1\rho(dd)}/R_1^{NS}]$ to eliminate the distant dependent terms, r^6.

In contrast, most biological macromolecules, i.e., DNAs, RNAs, proteins, carbohydrates, and lipids, belong to regime 3 ($\omega\tau_c \gg 1$). In this case, there are two complications to hamper the evaluation of $R_{1\rho(dd)}$. On one hand, the ratio $[R_{1\rho(dd)}/R_1^{NS}]$ for the macromolecules varies rapidly with subtle changes of values in τ_c (Figure 1) and is high, i.e., 68.6 for the B-(CG)$_3$ with τ_c = 5.0 ns and 42.3 for the Z-d(CG)$_3$ with τ_c = 3.9 ns. This leads to erroneous estimations of $R_{1\rho(dd)}$. On the other hand, the spin-diffusion predominates the spin-lattice relaxation processes of the DNA molecules in solution, as has been demonstrated by Kearns and co-workers,[11,26] so that the recovery of the R_1^S measurements is complicated. To extract meaningful information, R_1^{IS} must be used. Therefore, the dipolar contribution, $R_{1\rho(dd)}$, can be obtained as the product of R_1^{IS} and the corresponding ratio $[R_{1\rho(dd)}/R_1^{IS}]$.

Internal Motions of the B- and Z-d(CG)$_3$. It is necessary to specify the time scale when the dynamic properties of the molecules are discussed. Biological macromolecules may have totally dif-

(35) Unpublished results.

ferent mobilities at different time scales, and a certain motion at a specific time scale may be responsible for expressing their biological functions.

The internal motions detected by the $R_{1\rho}$ measurements for the B- and Z-d$(CG)_3$ in 2 M $NaClO_4$ solution are in the time range of $1/\omega_1$. The $R_{1\rho}$ measurements reveal the important features of the internal motions of these molecules. Both the B- and Z-d$(CG)_3$ have exchange contributions, $R_{1\rho(ex)}$, indicating that both molecules have the internal motions in this time range. However, the magnitude of $R_{1\rho(ex)}$ for the B- and Z-d$(CG)_3$ is markedly different (Table III). $R_{1\rho(ex)}$ for the Z-d$(CG)_3$ is 2-3 times larger than that for the B-d$(CG)_3$.

The larger exchange contribution, $R_{1\rho(ex)}$, to the overall relaxation rates, $R_{1\rho(obsd)}$, of the Z-d$(CG)_3$ may arise from large chemical shift differences between conformational states. An alternative explanation is the larger amount of lower frequency components in the Z-d$(CG)_3$. Preliminary results demonstrate that the exchange lifetimes are in the range of 10-20 μs for the B- and Z-d$(CG)_3$. $R_{1\rho}$ can be measured at different ω_1 fields, and the analysis of the ω_1 dependence of $R_{1\rho}$ will provide information of both the exchange lifetimes and the chemical shift differences between sites independently. The chemical shift differences are considered to correlate with the magnitude of the amplitudes of the internal motions.[19] Further work along this line is in progress.

Acknowledgment. This research was supported by the Research Corp. and the American Chemical Society, Illinois Division, Grant 87-30. We wish to thank Drs. K. D. Kopple and J. Longworth for inspiring discussion. We thank J. Bernhardt for many helpful suggestions.

Ultrafast Ligand Rebinding to Protoheme and Heme Octapeptide at Low Temperature

Jay C. Postlewaite, Jeffrey B. Miers, and Dana D. Dlott*

Contribution from the School of Chemical Sciences, University of Illinois at Urbana Champaign, 505 South Mathews Avenue, Urbana, Illinois 61801. *Received May 2, 1988*

Abstract: Ultrafast flash photolysis is used to investigate the rebinding of carbon monoxide to protoheme (PH) and heme octapeptide (HO) in a glycerol-water glass at 100 K. Kinetic decay data are obtained at several probing wavelengths in the Soret bands. Previous work [Hill, J. R., et al. *Springer Ser. Chem. Phys.* **1986**, *46*, 433] had shown the existence of two distinct ligand rebinding processes. The first, denoted process I*, is exponential in time, with a rate of $\approx 3 \times 10^{10}$ s^{-1}. Process I* involves non-Arrhenius rebinding, as evidenced by a roughly linear dependence of the rate constant on temperature. The second, denoted process I, involves nonexponential rebinding which does obey the Arrhenius expression for a system with distributed activation barriers. Kinetic measurements performed at the isosbestic point between carboxy heme (denoted Fe-L) and deoxy heme (denoted Fe + L) demonstrate the existence of two short-lived intermediates (denoted Fe^{I}--L and Fe*--L). Multiple-flash experiments at 15 K show that these species cannot be easily interconverted, implying they exist as two distinct, inhomogeneous sets of reacting molecules. One reacting subensemble consists of Fe-L species which, upon photolysis, relax at a rate of $\approx 10^{12}$ s^{-1} into Fe + L and then rebind ligands via process I. The other consists of molecules which are unable to relax into Fe + L states, and which rebind ligands via process I*. The difference between the two subensembles is attributed to solvent interactions which constrain the geometry of some molecules to inhibit the relaxation process. The rebinding parameters of PH and HO are compared at 100 K. The HO differs from PH by the addition of a basket handle peptide chain which donates a proximal histidine. HO relaxes faster (1 ps) after deligation than does PH (1.5 ps). Process I* rebinding to unrelaxed hemes has nearly the same rate in PH and HO. This observation is consistent with a picture of ligand rebinding to planar, unrelaxed hemes which differ only in proximal substitution. Process I is much slower in HO, probably because proximal tension exerted by the peptide chain on the relaxed heme increases the activation barrier.

The rebinding of photodissociated neutral ligands to heme[1-3] has received considerable attention because heme derivatives have important catalytic properties and play a central role in enzyme biochemistry. In this work we report ultrafast, multispectral kinetic data on rebinding of carbon monoxide to iron(II) protoheme (PH) and heme octapeptide (HO) at low temperature (T = 100 K) in a solvent glass (glycerol-water 75:25). In these low-temperature systems, photolyzed ligands are confined in a glassy solvent cage surrounding each heme. Geminate rebinding to Fe can be studied without the complications induced by migration through a protein matrix or diffusion through the solvent.[4-6]

The processes we study can be divided into three stages. In the first stage, photodissociation, every heme is bound to a ligand, carbon monoxide (CO), and is denoted as the Fe-L state. The Fe-L complex is nearly planar, with low spin, $S = 0$.[3,5] Upon photoexcitation, the ligand moves away from Fe along a repulsive potential surface. The short-lived intermediate formed by the photolysis process will be denoted Fe--L. The spin state(s) of such Fe--L species are unknown at this time. The second stage involves the relaxation of this intermediate into the stable deligated heme, denoted Fe + L. The Fe + L species is characterized by a domed heme with high spin, $S = 2$.[3,5] Finally, the third stage involves ligand rebinding which transforms Fe + L into Fe-L molecules.

Heme octapeptide is prepared by enzymatic digestion of cytochrome c,[7] and it differs from PH by the presence of a "basket

* Author to whom correspondence should be addressed.

(1) DeBrunner, P. G.; Frauenfelder, H. *Annu. Rev. Phys. Chem.* **1982**, *33*, 283.
(2) Frauenfelder, H.; Parak, F.; Young, R. D. *Annu. Rev. Biophys. Biophys. Chem.* **1988**, in press.
(3) Antonini, E.; Brunori, M. *Hemoglobin and Myoglobin in Their Reactions with Ligands*; North Holland: Amsterdam, 1971.
(4) Austin, R. H.; Beeson, K. W.; Eisenstein, L.; Frauenfelder, H.; Gunsalus, I. C. *Biochemistry* **1976**, *14*, 5355.
(5) Alberding, N.; Austin, R. H.; Chan, S. S.; Eisenstein, L.; Frauenfelder, H.; Gunsalus, I. C.; Nordlund, T. M. *J. Chem. Phys.* **1976**, *65*, 4701.
(6) Hill, J. R.; Cote, M. J.; Dlott, D. D.; Kauffman, J. F.; McDonald, J. D.; Steinbach, P. J.; Berendzen, J. R.; Frauenfelder, H. *Springer Ser. Chem. Phys.* **1986**, *46*, 433.
(7) Harbury, H. A.; Loach, P. A. *J. Biol. Chem.* **1960**, *235*, 3640.

0002-7863/89/1511-1248$01.50/0